Solid-State Electronics 105 (2015) 51–57

Contents lists available at ScienceDirect

Solid-State Electronics

journal homepage: www.elsevier.com/locate/sse

Effect of annealing temperature and X-ray irradiation on the performance of tetraphenylporphyrin/p-type silicon hybrid solar cell

M.M. Makhlouf [a,b,c,*], H.M. Zeyada [b]

[a] Department of Physics, Faculty of Applied Medical Sciences at Turabah Branch, Taif University, Turabah 21995, Saudi Arabia
[b] Department of Physics, Faculty of Science at New Damietta, Damietta University, New Damietta 34517, Egypt
[c] Department of Physics, Damietta cancer institute, Damietta, Egypt

ARTICLE INFO

Article history:
Received 7 November 2013
Received in revised form 3 November 2014
Accepted 27 November 2014

The review of this paper was arranged by Prof. E. Calleja

Keywords:
Heterojunction device
Photovoltaic properties
Annealing temperatures
X-ray irradiation dose

ABSTRACT

Hybrid organic–inorganic heterojunction solar cell, Au/tetraphenylporphyrin (TPP)/p-Si/Al, was fabricated. The TPP films were deposited by thermal evaporation technique onto p-type silicon single crystal wafer. The current–voltage characteristics of the heterojunction diode have been studied at a temperature range of 298 – 390 K and the voltage applied during measurements varied from -1.5 to 2 V. The device showed a rectification behavior like a diode under different temperatures. It was found that the conduction mechanisms of the diode are controlled by the thermionic emission at forward voltage bias $\leqslant$0.5 V and the single trap level space charge limited conduction (SCLC) mechanism at forward voltage bias >0.5 V. Dependence of the *I–V* characteristics on temperature, illumination and X-ray irradiation dose of 50 kGy for such a device have been studied. The dependence of photovoltaic parameters on annealing temperatures, illumination conditions and irradiation dose has been estimated. The calculated parameters are: series and shunt resistances, ideality factor, barrier potential, open-circuit voltage, short-circuit current, fill factor and efficiency.

1. Introduction

In recent years, there has been growing interest in the field of organic semiconductors due to their successful application in optical and electronic devices. However, up to the present time, most of fundamental properties of organic semiconductors have not yet sufficiently been clarified since most traditional measuring techniques developed for inorganic semiconductors are not necessarily applicable to them. In order to improve the performance of the organic devices, it is necessary to obtain a deep focus into chemical and physical properties of these organic semiconductors.

Porphyrin dyes are called pigments of life because they play an essential function in many biological processes starting from oxygen transport to photosynthesis and from catalysis to pigmentation changes. Moreover, they have an extended π-conjugation system that results in a wide range of wavelengths for light absorption and emission, charge generation and transport [1–3].

Porphyrins have excellent films that were prepared by chemical and physical methods, such as thermal evaporation, chemical vapor deposition, spin coating and Langmuir Blodgett techniques [4–9]. These films are used successfully in fabricating electroluminescent devices [10], photonic devices [11], solar energy conversion devices [12], photo-electro-chemical cell [13], optoelectronic devices [14] and gas sensors [15].

Tetraphenylporphyrin, TPP, has the chemical formula $C_{32}H_{42}N_4$. The basic structure of TPP is centro-symmetrical with two independent pyrroles and phenyl groups as shown in Fig. 1. TPP has an extended π-conjugation system with 24-π electron that results in a wide range of wavelengths for light absorption. The absorption spectra of TPP have been reported by using different techniques, such as Langmuir-Boledget films [16], thermoplastic media [17], solvents [18] and nematic crystals [19]. TPP absorbs visible light and then converts photo-energy into electrical and chemical energy. A great deal of effort has been exerted to study the optical properties of TPP because of its high optical absorption potential in UV–Vis. region.

Extensive research has been conducted for applying porphyrins compounds as semiconducting materials to obtain many electronic and photo-electronic devices by using heterojunction of

* Corresponding author at: Department of Physics, Faculty of Applied Medical Sciences at Turabah Branch, Taif University, Turabah 21995, Saudi Arabia. Tel.: +20 572700066, +966 547952264.
E-mail address: m_makhlof@hotmail.com (M.M. Makhlouf).

http://dx.doi.org/10.1016/j.sse.2014.11.020
0038-1101/

organic-organic and hybrid organic–inorganic structures. Some authors [20–22] have fabricated organic–inorganic devices to benefit from the advantages of both materials in a single device.

The application of TPP and its derivatives in solar cell manufacturing process will be provided as thin film sandwich. The sandwich may be constructed in homo- or hetero-junction configuration. Different homojunction cell structures utilizing TPP as a semiconductor were developed [23,24]. Indium tin oxide, ITO, sandwich-type cell, into which a long-chain tetraphenylporphyrin was injected without any metal ions in the central core has been constructed [23]. The current–voltage, *I-V*, characteristics exhibit a remarkable rectification behavior for both crystalline and low-temperature lamellar phases. The TPP layer, 25–65 nm in thickness, was deposited by molecular beam epitaxial on ITO substrates and covered by aluminum as a back contact. Transport and trapping of carriers and the occurrence of electrochemical phenomena in the device are studied by performing the *C–V* measurements at low frequencies [24]. Furthermore, metal–semiconductor interactions at the contacts are investigated when the signal frequencies are high in comparison with the carrier transit time in the device. Such homojunction devices have loss factors including: photo carrier generation is a function not only of bulk optical absorption, but also of available mechanisms for exciton dissociation, non-irradiative recombination at the interfaces and non-geminate recombination at impurities. Single layer solar cells of this type deliver quantum efficiencies of less than 1% and power conversion efficiencies of less than 0.1% [24].

In heterojunction solar cells, the local electric fields are strong and may break up photo generated exciton provided that the differences in potential energy are larger than the exciton binding energy. The organic donor–acceptor interface separates exciton much more efficiently than the organic -metal interface; efficient photovoltaic devices may be made from heterojunction solar cells. A heterojunction sandwich cell of $Al/Al_2O_3/MnTPP/Au$ was designed [25]. The photovoltaic efficiency of porphyrin compounds increases with decreasing film thickness from 200 to 100 nm [25].

In this work, the attention has been focused on fabricating a hybrid heterojunction device of Au/TPP/p-Si/Al and providing a complete investigation about its electronic transport mechanisms and photovoltaic properties. In addition, the influence of environmental conditions, such as temperature, illumination and high energy (6 MeV) X-ray irradiation on the efficiency of the solar cell has been reported.

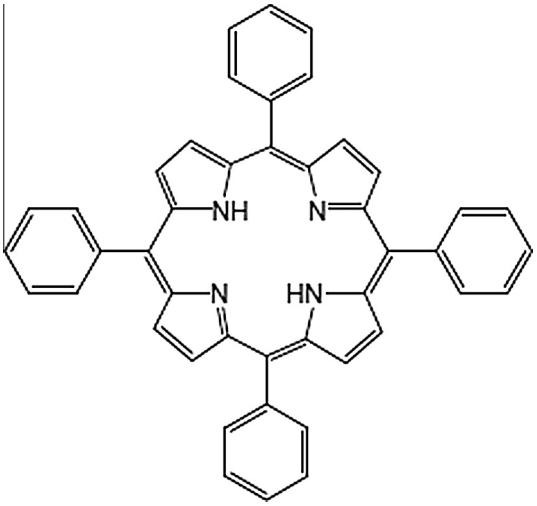

Fig. 1. Molecular structure of TPP.

2. Experimental techniques

Tetraphenylporphyrin, TPP, was purchased from Aldrich Chem. Co. with purity 99% and it was used in a powder form of as received condition without further purification. The hybrid junction of Au/TPP/p-Si/Al solar cell was fabricated by conventional thermal evaporation technique. The vacuum system used for this purpose is a high vacuum coating unit (type E306A, Edwards Co., England). The pressure inside the vacuum work chamber was pumped down to 1.5×10^{-5} Pa before starting the evaporation process. Evaporation of the material is carried out with quartz crucible heated by a tungsten heater. Rate of deposition (0.5 nm/s) and film thickness were controlled by using quartz crystal thickness monitor (model TM-350 Maxtek Inc. USA).

The cell has been prepared by using a polished p-type Si single crystal wafer with [100] orientation parallel to the surface, hole concentration of $1.6 \times 10^{23}\ m^{-3}$ and it's thickness is 400 μm. First, the p-Si wafer was chemically cleaned and etched by PC4 solution (HF: HNO_3: CH_3COOH in ratio 1:6:1) for 10 s, then rinsed with deionized water and isopropyl alcohol and oven-dried.

In designing such a device we took into consideration the factors influencing the photovoltaic properties in heterojunction solar cells [26]; namely optical filter effect, type of the dye and its thickness [26]. The optical filter effect of Au on TPP has been reduced by designing an Au mesh electrode instead of a continuous Au thin film electrode. TPP molecule has a good absorption in the UV–vis. range of spectra which is improved by annealing at 390 K for 2 hrs as will be shown in Fig. 3. The back contact was made by depositing a relatively thick film of pure Al to the bottom of p-Si substrate. TPP organic layer with thickness of 95 nm was deposited on the front surface of p-Si wafer. Then, a front contact of pure gold was evaporated on TPP layer as a mesh grid electrode. The active area of the junction is $1.65 \times 10^{-2}\ cm^2$. Fig. 2 shows a schematic diagram of hybrid heterojunction, Au/TPP/p-Si/Al, solar cell.

The current–voltage, *I-V*, characteristics of the pristine heterojunction device were measured under dark and illumination conditions for different annealing temperatures by using Keithly 617 electrometer. The incident power density of light illumination was 50 mW/cm^2 provided by tungsten lamp. The intensity of the incident light was measured by using a digital lux-meter (Lutron-Model LX-107).

These measurements were also performed for the heterojunction device after being exposed to high energy (6 MeV) X-ray. The irradiation dose was 50 kGy generated from linear accelerator (Philips Co., linac multi-energies model SL15).

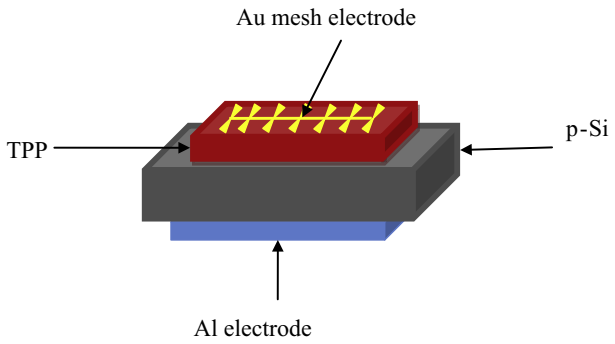

Fig. 2. A schematic diagram of the structure of Au/TPP/p-Si/Al solar cell.

3. Results and discussion

3.1. The absorption spectrum for TPP thin films

Fig. 3 illustrates the absorption spectra of the as deposited, annealed and irradiated TPP thin films. The highly conjugated tetraphenylporphyrin macrocycle of the as deposited film shows intense absorption termed Soret band that appeared in the wavelength range of 360–490 nm. The Soret band has two peaks, B_x and B_y, at 395 and 443 nm, respectively. Four additional weaker absorption bands termed Q bands is in the range of 500–720 nm. Those bands are superimposed on the absorption edge of TPP molecule. It is also noted that the bands B, N and M appear with intensities that are comparatively higher than of Q band, this is because absorption transitions in the Q-band region have small oscillator strengths due to opposite direction of the electric dipoles and the cancellation of electric dipoles that occurs leading to low intensity in the Q bands [27]. Annealing temperature results in an increase in the value of the absorption all over the spectra and a significant broadening of all absorption bands is observed. A red shift of Q-bands indicates the increase in π-conjugation due to increased planarity of TPP molecules and the decrease in the energy gap of TPP molecule. Exposing H_2TPP film to X-ray irradiation dose reduces the value of absorbance over all the spectra and influences peaks position in comparison with absorbance of the as-deposited and annealed ones. A blue shift is observed which will result in increasing the value of energy gap of TPP molecule.

3.2. The energy band diagram for TPP/p-Si heterojunction device

Depending on work functions (Φ_{Si}, Φ_{TPP}), electron affinities (Ψ_{Si}, Ψ_{Tpp}) and energy gaps (E_{Si}, E_{TPP}) of two semi conductors. The band profile of Si/TPP can be constructed. The work function is the energy to excite electron from Fermi level to the vacuum level, it is 4.97 eV for Si and can be calculated according to:

$$\Phi_{Si} = \Psi_{Si} + 0.56 + \frac{k_B T}{q} \ln \frac{N_a}{n_i} \quad (1)$$

where Ψ_{Si} = 4.1 eV [28], N_a is the concentration of acceptor atoms and n_i is the intrinsic concentration of carriers. Rojas [29] using tunneling spectroscopy determined the work function for TPP as 4 eV. Electron affinity, or the energy difference between vacuum and the bottom of conduction band, E_C, in Si or the bottom of (LUMO) in TPP, respectively. The larger electron affinity, the more energetically favorable it is to gain charge, and the easier it is for electrons to bind for the molecule. Ψ_{Tpp} is 1.68 eV [30]. As the TPP molecule is different from the Si atoms, the vacuum energy of the free molecule is not necessarily the same as the Si atoms. The interface results from the difference in the lattice parameter of both materials.

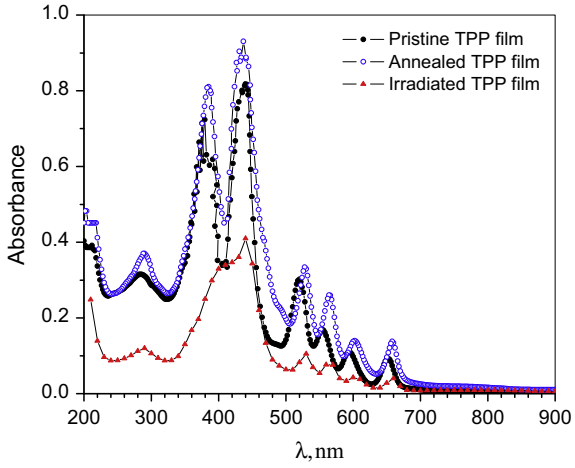

Fig. 3. The absorption spectrum for TPP thin films in as-deposited, annealed at 390 K for 2 h. and X-ray irradiated with a dose of 50 kGy.

The total built in voltage, V_D, is due to the difference in work functions (Φ_{Si}-Φ_{TPP} = 0.1 eV) is equal to the sum of built – in voltages on both sides ($V_D = V_{D,Si} + V_{D,TPP}$), $V_{D,TPP} = \Phi_{TPP}$-Ψ_{Tpp} = 0.77 eV and $\Delta E_v = (\Psi_{Si} + E_{g,Si}) - (\Psi_{Tpp} + E_{g,TPP})$ = 1.04 eV. The condition of constructed device is as follows:

$$V_{D,TPP} < \Delta E_v,\ \Phi_{Si} > \Phi_{TPP},\ \Psi_{Si} > \Psi_{Tpp},\ E_{g,Si} < E_{g,TPP} \text{ and } \Psi_{Si} + E_{g,Si} > \Psi_{Tpp} + E_{g,TPP} > \Psi_{Si}$$

Therefore, the band profile of Si/TPP heterojunction device can be constructed as shown in Fig. 4 [31].

Makhlouf, et al. [32] showed that TPP has HOMO-LUMO band gap of 2.45 eV and there are excitation bands available inside the energy-gap at various energy levels together with the localized energy states. At thermal equilibrium, the hole current density from Si to TPP equals the current density from TPP to the Si but with positive potential in the Si relative to TPP. The magnitude of the hole current density from the Si to TPP is greater than the current density from TPP to Si. The application of positive potential to Si steers the holes from Si to TPP. As a result, it is assumed that the bending profile of the valence band moves upward from the Si side indicating the lowering of the barrier.

3.3. Dependence of the I–V characteristics on temperature at dark conditions

Fig. 5 shows typical *I-V* characteristics of Au/TPP/p-Si/Al heterojunction diode in the temperature range 292–390 K where the applied bias potential varies from -1.5 V to 2 V during measurements. The results show that curves have the same *I-V* behavior. For the same applied voltage, current increases with increasing temperature, this indicates a negative temperature coefficient for the resistivity [33]. The results show also the existence of a weak leakage current in the reverse bias direction and it proves a good rectification performance for the diode. The rectification ratio, RR, is calculated as the ratio of the forward current to reverse current at a certain applied voltage. The RR values for the diode were calculated for different temperatures at ±1 V as shown in Table 1. The RR values increase with increasing annealing temperature and this indicates good performance of the device.

For theses curves, the forward current corresponds to the negative polarity on the Au electrode side. These curves are non-linear and this device clearly exhibits moderate rectifying behavior due to the injection of the charge carriers from the Al electrode to the device. The other diode parameters, such as series resistance, R_s, and shunt resistance, R_{sh}, were obtained at room temperature by the method stated in [34] by which we can calculate the junction resistance, R_J, by using the following relation:

$$R_J = \frac{\partial V}{\partial I} \quad (2)$$

The values of the series, R_s, and shunt, R_{sh}, resistances are determined by plotting the junction resistance R_J as a function of the forward and reverse bias potentials of the junction for each temperature. At the high forward voltages, the junction resistance reaches a constant value, which is equal to R_s. The same behavior also occurs in reverse bias voltages leading to determination of the value of R_{sh}. The determined values of R_s and R_{sh} at different temperatures are listed in Table 1. It has been noted that the values of R_s and R_{sh} decreases with increasing annealing temperatures.

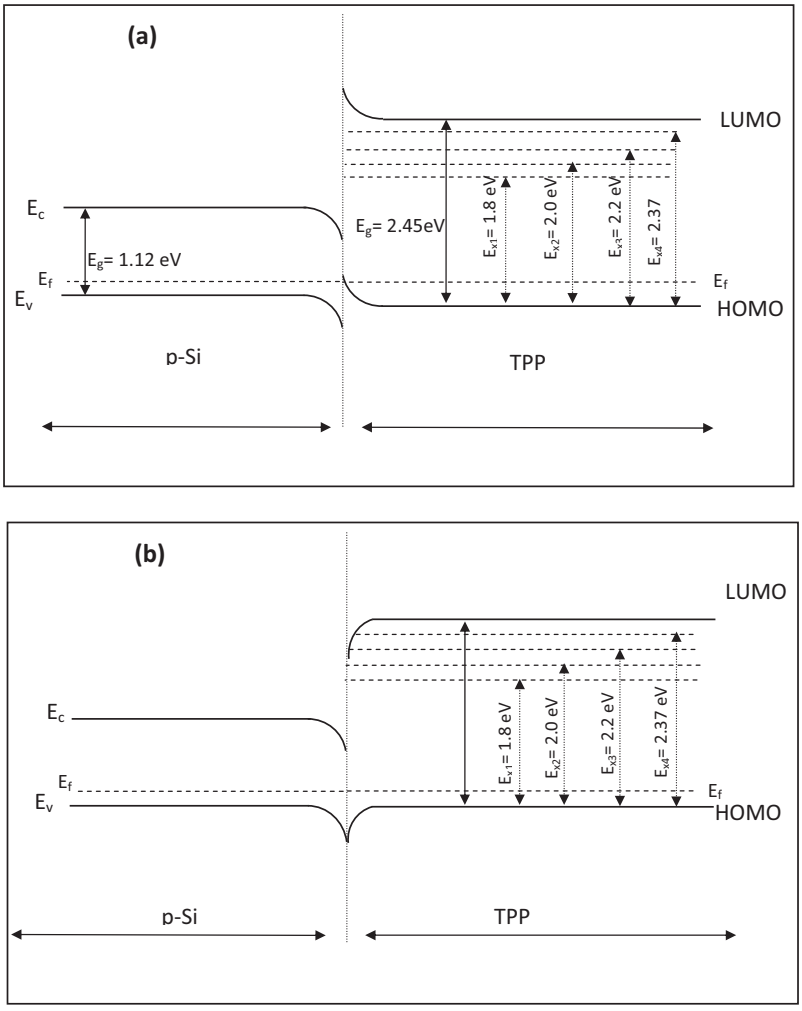

Fig. 4. Energy band diagram for TPP/p-Si hybrid heterojunction device (a) for forward bias smaller than energy gap and (b) modified profile due to the presence of charged interface.

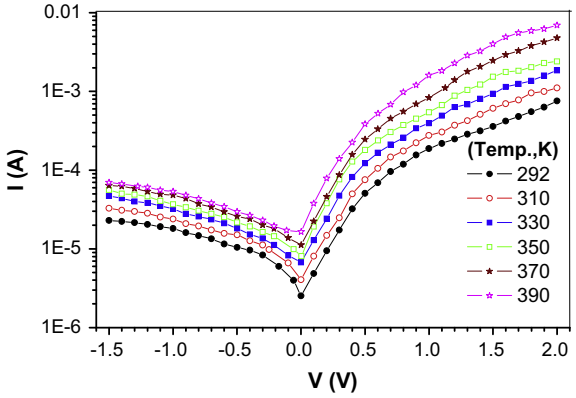

Fig. 5. *I–V* characteristics of Au/TPP/p-Si/Al heterojunction device in the dark at temperatures range 298–390 K.

In order to determine the operating conduction mechanisms in Au/TPP/p-Si/Al heterojunction device, we can use any one of the diffusion models, the emission model or the recombination model [33] in which a relation between I and V can be described. At low forward bias potential, $V \leqslant 0.5$ V. The relation between $\ln I$ versus V, at different temperatures in the range 298–390 K, is shown in Fig. 6. The logarithmic of the forward current of the diode increases linearly with the increase in bias potential. Thus, we can deduce

Table 1
Influence of annealing temperatures on the electrical parameters of Au/TPP/p-Si/Al solar cell.

T (K)	I_s (μA)	RR	R_s (Ω)	R_{sh} (kΩ)	n	Φ_B (eV)
292	6.6	12.3	4580	54.1	3.25	0.59
310	8.5	13.5	3030	40.5	3.10	0.62
330	11.1	16.0	2000	31.2	2.95	0.65
350	13.6	18.7	1420	25.7	2.80	0.69
370	16.9	23.9	833	21.3	2.51	0.73
390	19.0	36.7	500	19.1	2.50	0.76

that Au/TPP/p-Si/Al heterojunction device behaves like a Schottky diode. In that case, *I-V* characteristics of the diode can be analyzed by the following relation [35]

$$I = I_S\left(\exp\left(\frac{eV}{nk_BT}\right) - 1\right) \tag{3}$$

where n is the ideality factor, e is the electronic charge, k_B is the Boltzmann constant and I_s is the reverse saturation current given by the following relation [36]

$$I_S = AA^*T^2 \exp\left(\frac{-e\Phi_b}{k_BT}\right) \tag{4}$$

where A is the diode contact area, A^* is the Richardson constant (A^* = 32 A/cm^2 K^2 for p-Si [33]) and Φ_b is the barrier height. The ideality factor n is a measure of homogeneity of the interfacial layer

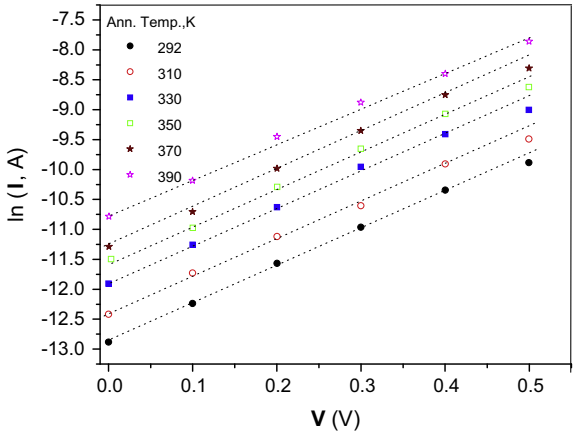

Fig. 6. Variation of ln$I$ versus V of Au/TPP/p-Si/Al heterojunction device for different temperatures at forward voltage <0.5 V.

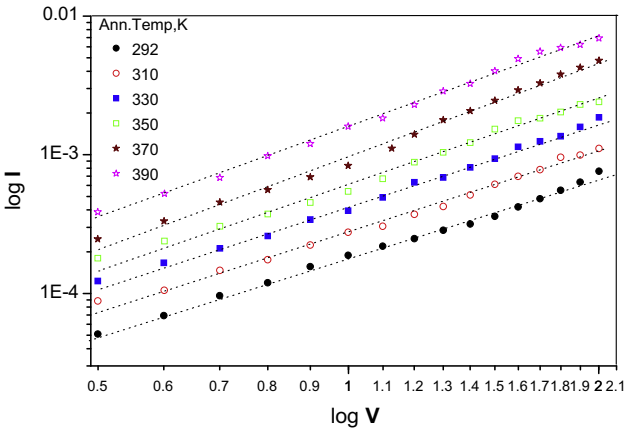

Fig. 8. Plot of log$I$ versus log$V$ of Au/TPP/p-Si/Al heterojunction device for different temperatures at forward bias potential >0.5 V.

between organic and inorganic semiconductors and it is determined from the slope of the linear relation of ln$I$ versus V in Fig. 6 through the relation:

$$n = \frac{e}{k_B T}\left(\frac{dV}{d(\ln I)}\right) \tag{5}$$

The obtained value of n is higher than unity indicating that the diode has nonideal behavior. The deviation of n from unity may be attributed to either recombination of electrons and holes in the depletion region or increase of diffusion current due to an increase of applied voltage [37].

The barrier height is calculated by using Eq. 3 in the following form:

$$\Phi_B = \frac{k_B T}{e}\left(\frac{AA^* T^2}{I_S}\right) \tag{6}$$

where I_s is obtained from the intercept of ln(I)–V curves with ordinates axis as illustrated in Fig. 6. The values of the barrier potential height and ideality factor as a function of temperatures are shown in Fig. 7. It is noted that the ideality factor decreases with the increase in temperature while the barrier height increases with increasing temperature. Such a behavior indicates presence of heterogeneous interface between TPP film and Si substrate.

At large forward voltage bias >0.5 V, the current as a function of the forward applied voltage is plotted in log–log scale as shown in Fig. 8. The current shows a power law dependence on potential of the form $I = V^m$ where m varies between 1.86 and 2.18 depending on temperature. This indicates that the current in the diode is controlled by single trap energy level space charge limited conduction (SCLC) mechanism. The current in such a mechanism is given by [38]

$$I = \frac{9}{8}\varepsilon\mu\left(\frac{N_c}{N_t}\right)\left(\frac{V^2}{d^3}\right)\exp\left(\frac{-E_t}{k_B T}\right) \tag{7}$$

where N_t is the concentration of traps at energy level E_t, over the valence band edge, N_c is the density of states in the valence band and $d = 95$ nm is the film thickness of TPP in this device. Fig. 9 shows the plot of ln(I) versus reciprocal temperature at a fixed bias potentials (1, 1.2 and 1.4 V) in SCLC region. In this region, the trap energy and the concentration of traps, N_t, can be calculated from the slope of straight lines and their intercept with ordinate axis. The calculations showed that they have values of 0.216 eV and 3.1×10^{24} m^{-3}, respectively. The values of N_t and E_t were calculated assuming that $N_v = 10^{21}$ cm^{-3} [38], $\varepsilon = 2.69 \times 10^{-13}$ F cm^{-1} and $\mu = 2.1 \times 10^{-2}$ cm^2 V^{-1} s^{-1} [39].

In reverse bias potential direction, the temperature dependence of Ln (I_R) at constant reverse bias potential is illustrated in Fig. 10. The linear relationship between the logarithm of reverse current and temperature indicates that the reverse current is thermally activated process and it varies exponentially with temperature. The relation governing such a behavior is given by [40]:

$$I_R = I_S \exp(-\Delta E/k_B T) \tag{8}$$

where ΔE is the activation energy and I_S denotes the reverse saturation current, from the slope of these straight lines the obtained average activation energy is 0.58 eV. This value is nearly equal to one half of the energy gap of Si substrate (1.1 eV), such a behavior indicates that the temperature and voltage dependence of the dark reverse current is governed by generation and recombination of charge carriers in Si substrate [41] rather than at organic–inorganic interface or organic material.

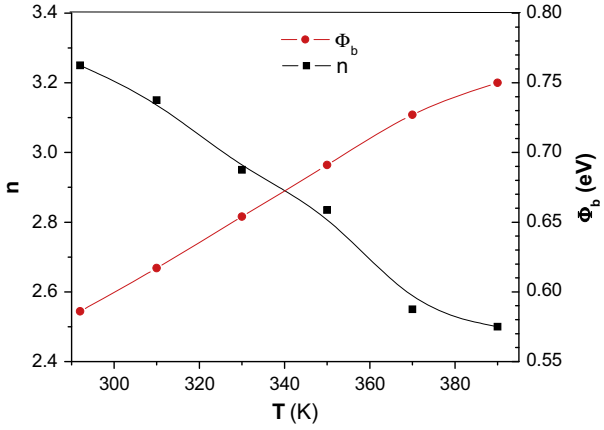

Fig. 7. Temperature dependence of ideality factor and barrier height of Au/TPP/p-Si/Al heterojunction device.

3.4. Photovoltaic properties of Au/TPP/p-Si/Al device under different environmental conditions

Fig. 11 illustrates I–V characteristic curves in dark conditions and under illumination for the virgin, annealed and irradiated Au/TPP/p-Si/Al heterojunction solar cell. The forward and reverse bias currents increased after annealing the virgin device at 390 K for 2 h. It was found that annealing of the device was required to complete and enhance its performance. Calculations of the electrical parameters of the solar cell indicated that annealing

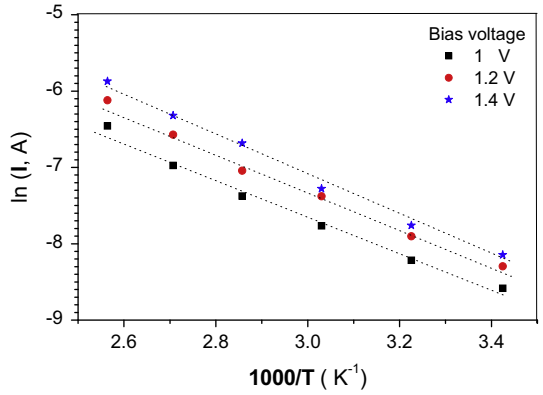

Fig. 9. Plot of log$I$ versus 1000/T at a fixed voltages of (1, 1.2 and 1.4 V) in the SCLC region of Au/TPP/p-Si/Al heterojunction diode.

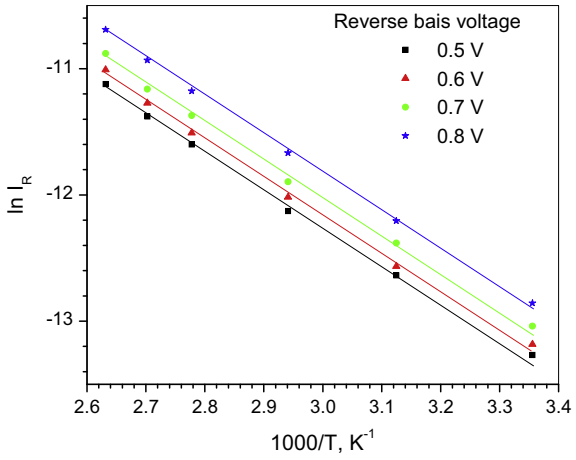

Fig. 10. Plot of lnI_R versus 1000/T at a fixed voltages of (0.5, 0.6, 0.7 and 0.8 V).

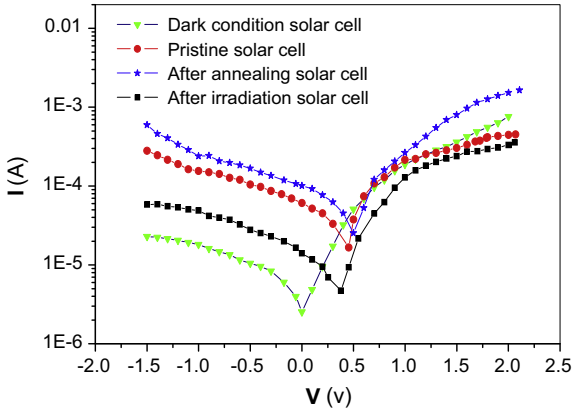

Fig. 11. I–V characteristics of Au/TPP/p-Si/Al solar cell under different conditions for: (▼) dark condition, (●) Virgin fabricated device, (★) Annealed device at 390 K for 2 hrs (■) Exposed to X-ray of dose 50 kGy.

temperatures increased the saturation current, rectification ratio and barrier potential and decreased the series and shunt resistances and the ideality factor (Table 1). Liu et al. [42] optimized the annealing temperature (150 °C for 2 h) to produce a device (P3HT and silicon nanocrystals) with improved PCE of 1.47%. An increase of both I_{sc} and fill factor is achieved as a result of annealing. This is attributed to an increase in hole mobility, which leads to a more balanced device mobility. This causes a reduction in the build-up of space charge and a reduction in recombination [43].

Table 2
Photovoltaic parameters of Au/TPP/p-Si/Al solar cell versus annealing temperatures and x- ray irradiation dose.

Solar cell device condition	V_{oc} (V)	I_{sc} (μA)	$P_M \times 10^{-6}$ (W)	Fill factor (FF)	Efficiency (η%)
Pristine	0.45	61	9.64	0.35	1.17
Annealed	0.50	100	17.9	0.35	2.13
Irradiated	0.39	15.2	2.37	0.37	0.27

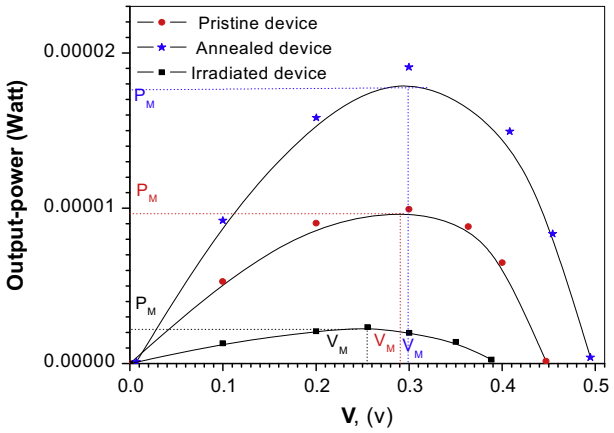

Fig. 12. The output power versus voltage for (●) A virgin, (★) Annealed and (■) Irradiated Au/TPP/p-Si/Al solar cell.

Exposing the device to an irradiation dose of 50 kGy resulted in a large decrease of diode photovoltaic parameters (Table 2). The X-ray irradiation has an effect on the excitonic and impurities levels, this will result in the change in the microstructure of the junction. An increase in series resistance indicates that both of the mobility and the free carrier concentration has decreased. The reduction in mobility is due to the introduction of defect centers with irradiation which act as scattering centers and the free carrier concentration will be reduced if deep traps are introduced into material associated with point defect damage [44,45].

The total current under illumination can generally be described by [46]:

$$I = I_{ph} - I_s\left(\exp\left(\frac{eV}{nk_BT}\right) - 1\right) - \left(\frac{V + IR_s}{R_{sh}}\right) \tag{9}$$

where I_{ph} is the component of the current that has been generated by illumination. The effect of illumination on the power–voltage characteristics of the device is depicted in Fig. 12. The values of the short circuit photocurrent, I_{sc}, open circuit voltage, V_{oc}, are listed in Table 2. The fill factor, FF, and the power conversion efficiency, η, of the device are given by [47,48]

$$FF = \frac{V_M I_M}{V_{oc} I_{sc}} \tag{10}$$

$$\eta = \frac{V_{oc} I_{sc}}{AP_{in}} FF \times 100\% \tag{11}$$

where I_M, V_M are the current and voltage at maximum power point, respectively and A is the active area of the junction. Various photovoltaic parameters obtained after illumination, annealing and X-ray exposure on the device are listed in Table 2. It is noted that there are changes in the cell parameters due to annealing and irradiation processes. Annealing temperature removes traps and defects from the band energy gap of TPP and decreases its value as shown in Fig. 3, therefore, the photo current of the device increased. Annealing temperature at 390 K for 2 h increased the value of open circuit voltage (V_{oc}), short circuit current (I_{sc}) and the voltage (V_M) and the current

Table 3
Photovoltaic parameters of some hybrid solar cells based on TPP and its metal derivatives.

Solar cell construction	J_{SC} (mA/cm^2)	V_{OC} (Volt)	Fill factor (FF)	Efficiency (η%)	Refs.
Au/TPP/n-Si/Al	2.76	0.25	0.37	2.45	[50]
Au/ TPP/p-Si/Al	6.2	0.5	0.35	2.13	Present work
Au/ ZnTPP/p-Si/Al	2.3	0.22	0.24	2.24	[51]
Al/TPP/Mc/Au	–	0.99	0.27	0.33	[52]
Al/TPP/Mc(COOH)/Au	–	0.75	0.27	0.6	[52]
Al/TPP/Zn TPP/Au	–	0.51	0.38	2.7	[52]
Al/FeTPPCl/ p-Si /Al	2.8	0.47	0.32	5.6	[53]

(I_M) at maximum power point, as a direct consequence, the conversion efficiency increased. By irradiating the device with X-ray dose of 50 kGy, a decrease in the values of the cell parameters (Table 1) and a remarkable reduction in the values of (I_{sc}, V_{oc}, P_M and η) are observed (Table 2). Such a behavior can be explained on the basis of radiation induced defects in the surface and in the bulk of the solar cell. These defects compensate the positive charges at the TPP-Si interface and consequently decrease the output parameters of the solar cell [49]. Table 3 collects the results of photovoltaic parameters of some hybrid solar cells based on TPP and its metal derivatives. As it is clear from Table 3; the type of organic compound, the Si substrate and the combination of organic/organic compounds greatly influence the solar cell parameters.

4. Conclusions

Organic inorganic heterojunction device was fabricated. TPP as organic acceptor material is coated over p-Si substrate as inorganic acceptor material by thermal evaporation process to obtain Au/TPP/p-Si/Al bulk heterojunction solar cell. The *I- V* characteristics of the devices are taken in dark, illumination and also under high energy X-ray irradiation. The thermionic emission and the single trap energy level space charge limited current mechanisms were used to explain the *I-V* behavior in the forward bias for such a device. The diode parameters, such as the rectification ratio, the ideality factor, series and shunt resistances and the barrier height were calculated. In reverse bias direction; generation and recombination of holes in Si substrate are responsible for reverse current. The Au/TPP/p-Si/Al solar cell showed reasonable power conversion efficiency after annealing process at temperature of 390 K. Annealing temperatures increased the saturation current, rectification ratio and barrier potential and decreased the series and shunt resistances and the ideality factor, as a direct consequence there is an increase in charge carrier mobility, a decrease in the rate of recombination of the charge carriers, increase in charge carrier concentration, photocurrent and efficiency. On the other hand, power conversion efficiency of that cell decreases after being exposed to 6 MeV X-ray irradiation. This is due to the creation of radiation induced defects at the interface of the structure through the change in carrier concentration and carrier mobility. Photovoltaic parameters like open-circuit voltage, short-circuit current, fill factor and conversion efficiency were obtained.

Acknowledgment

This work was supported by the vice-Presidency of graduate studies and academic research (Taif university – Saudi Arabia); it is gratefully acknowledged.

References

[1] Nielsen KA, Levillain E, Lynch VM, Sessler JL, Jeppesen JO. Chem Eur J 2009;15:506.
[2] Kobayashi N, Janda P, Lever ABP. Inorg Chem 1992;31:5172.
[3] Neghabi M, Behjat A, Mirjalili BiBiF, Zamani L. Curr Appl Phys 2013;13:302.
[4] Takag T, Hooshino A, Miyaji H, Izumi K, Kokawa R. Jpn J Appl Phys 2001;40:6929.
[5] Snow AW, Jarvis NL. J Am Chem Soc 1984;106:4706.
[6] Paolesse R, Di Natale C, Macagnano A, Fabrizio D, Tristano B. Sens Actuor B 1998;47:70.
[7] Spadavecchia J, Rella R, Siciliano P, Manera MG, Alimelli A, Paolesse R, et al. Sens Actuor B 2006;115:12.
[8] Shinmori H, Kasiwara T, Osaka A. Tetrahedron Lett 2001;42:3617.
[9] Jia SL. Axial ligation and photo physical properties of non-planar Nikel (II) porphyrins. Ph.D. University of New Mexico, USA; 1999.
[10] Zhong G, Wu J, Wang Y, Li R, Xu J, Jianzhong. Thin Solid Films 2009;517(11):3340.
[11] Wróbel D, Siejak A, Siejak P. Sol Energy Mater Sol Cells 2010;94(3):492.
[12] Xiang Na, Zhou W, Jiang S, Deng L, Liu Y, Tan Zhuo, et al. Sol Energy Mater Sol Cells 2011;95(4):1174.
[13] Seo KD, Lee MJ, Song HM, Kang HS, Kim HK. Dyes Pigm 2012;94(1):143.
[14] Han W, Durantini E, More TA, Gust D, Petal R. J Phys Chem B 1997;101:1019.
[15] Muthukumar P, John SA. Sens Actuor B 2011;159(1):238.
[16] Grieve MB, Hudson AJ, Richardson T, Johnstone RA, Sobral AJ, Rocha AM. Thin Solid Films 1993;243:581.
[17] Sayo K, Deki S, Naguchi T, Goto K. Thin Solid Films 1999;349:276.
[18] Harime Y, Kodaka T, Price P, Eguchi T, Yamashieta K. Thin Solid Films 1997;307:208.
[19] Wróbel D, Goc J, Ion RM. J Mol Struct 1998;450:239.
[20] Güllü Ö, Türüt A. Sol Energy Mater Sol Cells 2008;92:1047.
[21] Gupta RK, Ghosh K, Kahol PK. Curr Appl Phys 2009;9:933.
[22] Karimov KhS, Ahmed MM, Moiz SA, Fedorov MI. Sol Energy Mater Sol Cells 2005;87:61.
[23] Shimizu Y, Shikawa AI, Kusabayashi S. Chem Lett 1986:1041.
[24] Pinotti E, Sassella A, Borghesi A, Paolesse R. Synth Met 2003;138:15.
[25] Nevin WA, Chamberiain GA. J Appl Phys 1991;69:4324.
[26] Takahashi K, Nakatani S, Komura T, Ito S, Murata K. Sol Energy Mater Sol Cells 1997;45:127.
[27] Baerends EJ, Ricciard G, Rosa A, Van Gisbergen SJ. Coord Chem Rev 2002;230:5.
[28] Neamen DA. "Semiconductor physics and devices" basic principles. 2nd ed. The Mc Graw Hill Companies Inc.; 1992 and 1997. p. 310.
[29] Rojas G. Self assembly and interface chemistry of non- metallated tetraphenyl porhyrin. Theses, Dissertations and Student Research: Department of Physics and Astronomy, University of Nebraska-Lincoln; 2011.
[30] Dabo I, Ferretti A, Park C-H, Poilvert N, Li Y, Cococcioni M, et al. Cond Mat Mater Sci 2012;7:1. Dec.
[31] Sharma BL, Puroth RK. Semiconductor heterojunctions. 1st ed. Pergamon Press; 1974. p. 34.
[32] Makhlouf MM, El-Denglawey A, Zeyada HM, EL-Nahass MM. J Lumin 2014;147:202.
[33] Sze SM. Physics of semiconductor devices. New York: Wiley; 1981. p. 97.
[34] Darwish S, Riad AS, Soliman HS. Semicond Sci Technol 1996;11:96.
[35] Yahia IS, Sakr GB, Wojtowicz T, Karczewski G. Semicond Sci Technol 2010;25:95001.
[36] Uslu H, Altindal S, Aydemir U, Dokme I, Afandiyeva IM. J Alloys Compd 2010;503:96.
[37] Yakuphanoglu F. Phys B 2007;388:226.
[38] Gould RD. J Appl Phys 1982;53:3353.
[39] El-Nahass MM, Zeyada HM, Abd-El-Rahman KF, Darwish AAA. Sol Energy Mater Sol Cells 2007;91:1120.
[40] Ahmed MM, Karimov KhS, Moiz SA. IEEE Trans Electron Dev 2004;51:121.
[41] Forrest SR. J Phys: Condens Mater 2003;15:S2599.
[42] Liu C-Y, Holman ZC, Kortshagen UR. Nano-Letters 2008;9:449.
[43] Liu C-Y, Holman ZC, Kortshagen UR. Adv Funct Mater 2010;20:2157.
[44] Aydogan S, Türüt A. Rad Phys Chem 2011;80:869.
[45] Pattabi M, Krishnan S, Ganesh S, Mathew X. Sol Energy 2008;81:111.
[46] Cong HN, Dieng M, Sene C, Chartier P. Sol Energy Mater Sol Cells 2000;63:23.
[47] Kilicoglu T, Ocak YS. Microelectr Eng 2011;88:150.
[48] Ashok S, Pandf KP. Sol Cells 1997;45:127.
[49] Neuhaus H, Hezel P. In: Proceedings of the 2nd world conference on photovoltaic solar energy conversion, Austria; 1998. p. 194.
[50] El-Nahass MM, Zeyada HM, Aziz MS, Makhlouf MM. Thin Solid Films 2005;492:290.
[51] Zeyada HM, El-Nahass MM, Ali MA. Eur Phys J Appl Phys 2011;56:10201.
[52] Takakashi K, Nakatani S, Yawaguichi T, Komura T, Ito S, Murota K. Sol Energy Mater Sol Cells 1997;45:127.
[53] El-Nahass MM, Metwally MS, EL-Sayed HEA, Hassanien AM. Synth Met 2011;161:2253.